Structural Elucidation and In Vivo Anti-arthritic Activity of β-Amyrin and Polpunonic Acid Isolated from the Root Bark of Ziziphus abyssinica HochstEx. A Rich (Rhamnaceae)

Article *in* Bioorganic Chemistry · March 2020

DOI: 10.1016/j.bioorg.2020.103744

CITATIONS
2

READS
236

10 authors, including:

Isaac Tabiri Henneh
University of Cape Coast
19 PUBLICATIONS **38** CITATIONS
SEE PROFILE

Boshi Huang
Virginia Commonwealth University
47 PUBLICATIONS **572** CITATIONS
SEE PROFILE

Faik N Musayev
Virginia Commonwealth University
68 PUBLICATIONS **1,154** CITATIONS
SEE PROFILE

Martin Safo
Virginia Commonwealth University
165 PUBLICATIONS **3,441** CITATIONS
SEE PROFILE

Structural Elucidation and *In Vivo* Anti-arthritic Activity of *β*-Amyrin and Polpunonic Acid Isolated from the Root Bark of *Ziziphus abyssinica HochstEx. A Rich (Rhamnaceae)*

Isaac T. Henneh,[a,1] Boshi Huang,[b,1] Faik N. Musayev,[b,c] Rana Al Hashimi,[b,c] Martin K. Safo,[b,c] Francis A. Armah,[d] Elvis O. Ameyaw,[d] Christian K. Adokoh,[e] Martins Ekor,[a,*] Yan Zhang[b,*]

[a]*Department of Pharmacology, School of Medical Sciences, University of Cape Coast, P.M.B. University Post Office, Cape Coast, Ghana*

[b]*Department of Medicinal Chemistry, School of Pharmacy, Virginia Commonwealth University, 800 E Leigh Street, Richmond, VA 23298, United States*

[c]*The Institute for Structural Biology, Drug Discovery and Development, School of Pharmacy, Virginia Commonwealth University, 800 East Leigh Street, Richmond, VA 23298, USA*

[d]*Department of Biomedical Sciences, School of Allied Health Sciences, University of Cape Coast, P.M.B. University Post Office, Cape Coast, Ghana*

[e]*Department of Forensic Sciences, School of Biological Sciences, University of Cape Coast, P.M.B. University Post Office, Cape Coast, Ghana*

---

[1] I.T,H. and B.H. contributed equally to this work.

[*]Corresponding authors. E-mail: m.ekor@uccsms.edu.gh. Phone: 23-3247950762 (M.E.). E-mail: yzhang2@vcu.edu. Phone: 1-804-8280021 (Y.Z.).

Abstract

Two natural products, compounds **1** and **2** were isolated from the root bark of *Ziziphus abyssinica* for the first time and were structurally elucidated as *β*-amyrin and polpunonic acid, respectively. Both compounds were further subjected to an *in vivo* study in rats to evaluate their anti-arthritic potency. Compared to the arthritic control group, rats treated with different doses of **1** or **2** (3, 10, and 30 mg/kg) exhibited significantly higher total change in body weight as well as lower arthritic scores and total change in paw edema and erythema. Histopathological examinations of the hind paws of the rats further demonstrated the beneficial effects of both compounds as they significantly reversed cartilage erosion, subchondral cyst, and Weichselbaum's lacunae formation. Evidence of bone remodeling was also observed in all groups of rats treated with **1** or **2**. Hematological and serum biochemical parameters were not significantly affected by treatment of **1** or **2**. Taken together, the results from the present study suggest potential therapeutic benefit of *β*-amyrin and polpunonic acid in rheumatoid arthritis and related inflammatory disorders.

Keywords

Ziziphus abyssinica; *β*-Amyrin; Polpunonic acid; Structural elucidation; Anti-arthritic activity

1. Introduction

Rheumatoid arthritis (RA), a common chronic inflammatory disorder, is a primary source of debility of the work force around the world[1]. About 1% of the population

in the world, mainly females, are affected with the severity of this disease[2].Although the exact etiology of the disease still remains unclear, severe inflammation in synovial joints occurs when the normally delicate synovial membrane becomes infiltrated with mononuclear phagocytes, lymphocytes, and neutrophils. Patients usually develop difficulties in mobility in the late stage of the disease, due to progressive dysfunction of cartilage and bones around the joints[2, 3].

Steroidal and non-steroidal anti-inflammatory drugs which are mostly used in the treatment of RA can ameliorate the symptoms of the disease. However, they only offer temporary relief, and also cause severe adverse effects, such as gastrointestinal bleeding, renal impairment, and immune-suppression[4, 5]. Because of these reasons, patients suffering from acute or chronic inflammatory disorders are prone to seeking alternative methods for relief and are among the highest users of complementary and alternative medicines, particularly herbal medications[6].

Ziziphus abyssinica (Hochst Ex A. Rich), a member of the Rhamnaceae family, is a well-known medicinal plant widely distributed in the tropical and warmer regions of the world[7]. It is commonly called ‘larukluror’ (Sisaala, Ghana) and ‘catch thorn’ (English)[8]. Previous studies have demonstrated that extracts ofthis plant possess antioxidant, antibacterial[9-11], antiplasmodial[12], anti-ulcerogenic [13], and anti-diarrhoeal[14] activities. Recently, we reported on the phytochemical composition of *Ziziphus abyssinica* and validated its ethnomedicinal use in pain management. The anti-nociceptive activity of the hydro-ethanolic leaf extract was believed to be mediated *via* inhibition of tumor necrosis factor (TNF-α), interleukin-1 beta (IL-1β), bradykinin and

prostaglandin E_2[15, 16]. Preliminary studies in our lab have also showed that extracts of the plant's root bark exhibited significant anti-inflammatory activity in several *in vitro* and *in vivo* models of acute inflammation[17].

To the best of our knowledge, there have been no reports on the isolated compounds of this plant, nor on their anti-arthritic activity in *in vivo* models of chronic inflammation. As we mentioned before, rheumatoid arthritis constitutes a significant disease worldwide, and effective treatment for the condition still remains a challenge. In the present study, we report the isolation, structure determination, and anti-arthritic activity of two triterpene-type natural products,compounds **1** (*β*-amyrin) and **2** (polpunonic acid) from the root bark of *Ziziphus abyssinica*.

2. Experimental

2.1. Plant collection

Fresh root bark of *Ziziphus abyssinica* was collected from Ejura (7.2300°N, 1.2200°W) in the Ashanti Region of Ghana in November, 2016. It was authenticated at the Herbarium Unit of the Faculty of Pharmacy of the Kwame Nkrumah University of Science and Technology (KNUST). A voucher specimen (KNUST/HM/2016/R003) was subsequently deposited at the herbarium.

2.2. Extraction

Fresh root bark of *Ziziphus abyssinica* were air dried at room temperature for three weeks and were pulverized into fine powder with the aid of a hammer mill. A portion

(800 g) of the powdered roots was defatted with 2 L of petroleum ether using a Soxhlet Apparatus (Aldrich®, St. Louis, MO, USA) at 50 °C. The defatted plant sample was dried and sequentially extracted with chloroform and 70% (v/v) methanol. The filtrates obtained were separately concentrated using a rotary evaporator (Rotavapor R-215 model, BÜCHI Labortechnik AG, Flawil, Switzerland) under reduced pressure at 50 °C. The residues were further dried in a desiccator containing activated silica to obtain a yield of 5.8% and 7.4% (w/w) for the chloroform and aqueous methanol fractions respectively.

2.3. Activity-guided isolation

A preliminary activity-guided isolation using the carrageenan-induced paw edema model in rats revealed the chloroform fraction was more potent than the methanol portion. A portion (35 g) of the chloroform fraction was loaded onto a chromatography column (60 cm × 3 cm) packed with silica gel (70-230 mesh), and then was eluted with gradient mixture of petroleum ether and ethyl acetate. 225 fractions were collected in 60 mL aliquots and bulked together into five sub-fractions based on their TLC profiles. Two fractions (21-27 and 125-150, respectively) were found to be more active and thus were further purified using petroleum ether. After showing single spot each on TLC plate, the compounds were recrystallized with acetone. This resulted in the needle-like crystal **1** (1.030 g)and shiny crystal **2** (1.642 g).

2.4. Structural identification

^{1}HNMR (400 MHz)and ^{13}CNMR (100 MHz) spectra were obtained at ambient temperature with tetramethylsilane (TMS) as the internal standard on a Bruker

Ultrashield 400 Plus spectrometer (Bruker, Germany). Chemical shifts were expressed in δ units (ppm), and J values were reported in hertz (Hz). HRMS spectra were acquired from a PerkinElmer Flexar UHPLC with AxION 2 Time of Flight (TOF) Mass Spectrometer (PerkinElmer, USA). Infrared (IR) spectroscopy were recorded on a Nicolet iS10 FTIR Instrument (Thermo Scientific, USA). Specific rotation ([α]) analysis was performed on a JASCO P-2000 digital polarimeter (JASCO, USA).

β-Amyrin (**1**): needle-like crystals; IR (Diamond, cm^{-1}): 3253; ^{1}HNMR (400 MHz, $CDCl_3$) δ: 5.18 (t, J = 3.56 Hz, 1H), 3.22 (dd, J_1= 10.84 Hz, J_2= 4.56 Hz, 1H), 0.79 (s, 3H), 0.83 (s, 3H), 0.87 (s, 6H, 3H × 2), 0.94 (s, 3H), 0.97 (s, 3H), 1.00 (s, 3H), 1.14 (s, 3H); see Table 1 for ^{13}CNMR (100 MHz, $CDCl_3$); HRMS *m/z* 449.3800 $[M+Na]^+$ (calculated for $C_{30}H_{48}O_3Na$, 449.3759).

Polpunonic acid (**2**): shiny crystals; $[\alpha]^{24}_D$−38.45 (*c* 0.07, $CHCl_3$); IR (Diamond, cm^{-1}): 3532, 3435, 3300, 2500, 1726, 1663; ^{1}HNMR (400 MHz, $CDCl_3$) δ: 0.72 (s, 3H), 0.86 (s, 3H), 0.88 (s, 6H, 3H × 2), 1.00 (s, 3H), 1.10 (s, 3H), 1.26 (s, 3H); see Table 1 for ^{13}CNMR (100 MHz, $CDCl_3$); HRMS *m/z* 479.3512 $[M+Na]^+$ (calculated for $C_{30}H_{48}O_3Na$, 479.3501).

2.5. X-ray crystallography.

Compound **2** was recrystallized from methylene chloride. A single crystal of $C_{30}H_{48}O_3 \cdot H_2O$ with approximate dimensions 0.155 mm × 0.375 mm × 0.501 mm was used for diffraction data collection at 100K using Rigaku MicroMax-007HF X-ray Generator, Eiger R 4M Detector and Oxford Cobra Cryo-system (Rigaku, Japan). The

diffraction data was processed by using CrysAl is PRO program[18]. Crystal belonged to the monoclinic C2 space group with cell dimensions: a = 13.33700(7) Å, b = 6.31317(4) Å, c = 30.75651(15) Å, β = 100.3632(5)°, Z = 4, volume = 2547.41(2) Å^3. Integration of the data yielded a total of 44153 reflections to a maximum θ angle of 67.05° (0.84Å resolution), of which 4335 were independent (completeness = 100%, Rint = 2.28%, Rsig = 0.0093%), and 4331 were greater than 2σ(F2). The final Data were corrected for absorption effects using the multi-scan method (SADABS).The structure was solved with the SHELXT[19] structure solution program using Intrinsic Phasing and refined with the olex2.refine[20, 21] refinement package using Gauss-Newton minimization. H atoms were determined from a difference Fourier synthesis. The final difference Fourier maps showed no peaks of chemical significance. The final anisotropic full-matrix least-squares refinement on F2 with 318 variable converged at R1 = 2.67%, for the observed data and wR2 = 7.22% for all data. The goodness-of-fit was 1.041. The largest peak in the final difference electron density synthesis was 0.13 e$^-$/Å^3 and the largest hole was -0.19 e$^-$/Å^3. On the basis of the final model, the calculated density was 1.2377 g/cm^3 and F(000), 1051.0 e$^-$.OLEX2 was used in molecular graphics and also used to prepare material for publication. Crystallographic data and structural refinement parameters for compound **2** is given in Table 2. Crystallographic data have been deposited with the Cambridge Crystallographic Data Centre (CCDC) with the accession number CCDC 1909815. This data is available from the CCDC *via* www.ccdc.cam.ac.uk/datarequest/cif.

2.6. Experimental design for in vivo anti-arthritic activity

Forty-five Sprague-Dawley rats (175-250 g) of both sexes were purchased from Noguchi Memorial Institute for Medical Research, University of Ghana, Legon-Ghana. The animals were kept under normal laboratory conditions with regards to room temperature, humidity, food and water. All protocols used in the study were in accordance with the NIH Guidelines for the Care and Use of Laboratory Animals and were approved by the Department of Biomedical Sciences, University of Cape Coast. Ethical approval for the study was obtained from the University of Cape Coast Institutional Review Board (UCCIRB), ID: UCCIRB/CHAS/2016/13, University of Cape Coast, Cape Coast, Ghana. Effects of test compounds (**1**and **2**) on chronic inflammation were evaluated using the adjuvant-induced arthritis animal model as previously described[22]. An aliquot (0.1 mL) of complete Freund's adjuvant (CFA) was intraplantarly injected into the right hind paws of rats. Arthritic control group received only intraplantar injection of CFA, whilst non-arthritic control group received only intraplantar injection of 0.1 mL of incomplete Freund's adjuvant (IFA) (that is sterile paraffin oil and water). Test groups received dexamethasone (3 mg/kg, *p.o.*), **1** (3, 10, 30 mg/kg, *p.o.*) and **2** (3, 10, 30 mg/kg, *p.o.*) once every day from day 14 to day 28.

2.7. Body weight change

Changes in body weight were determined every other day in all treatment groups till day 28. Percentage change in weights were calculated for each animal using the equation below from which time-course curves were plotted. The total areas under these

curves were estimated as the total change in body weight (AUC) over the entire duration of the test.

% Change in body weight = $(W_t\text{-}W_0/W_0) \times 100\%$, where W_t is the weight of the rats at day t, W_0 is the weight at day 0.

2.8. Paw thickness

Paw edema was measured using Starrett 798A – 6/150 Electronic Digital Calipers in both the ipsilateral (injected hind paw) and the contralateral paw (non-injected hind paw) before intraplantar injection of CFA (day 0) and on every other day up to the 28th day. Raw scores for ipsilateral and contralateral foot volumes were normalized individually as percentage of change from their values at day 0 and then averaged for each treatment group. Percentage of change in paw edema was calculated using the formula:

% Change in paw edema = $[(D_t\text{-}D_0)/D_0] \times 100\%$, where D_t is the paw diameter at day "t" and D_0 is the paw diameter before adjuvant injection. Data were presented as the effect of tested compounds on the time course curves and the total edema response was calculated in arbitrary units as the area under the curve (AUC) for 28 days.

2.9. Arthritic index

On day 29, the severity of arthritis was graded according to the extent of edema and erythema of the periarticular tissues [23], using a scale of 0-4 per limb, where 0 = no inflammation, 1 = mild inflammation of one joint of the paw, 2 = mild inflammation of

at least two joints of the paw, or moderate inflammation of one joint; 3 = severe inflammation of one or more joints; and 4 = maximum inflammation of one or more joints in the paw (gross deformity and inability to use the limb). The score for each paw were then added to get the total arthritis score (maximum possible score 16 per rat). The mean score for each treatment group was then designated as the arthritic index.

2.10. Photography

Photographs of the affected hind limbs were taken on day 29 using a digital camera (FE-5050, OLYMPUS, Tokyo, Japan).

2.11. Radiographic assessment

On the 29th day, all rats were anesthetized by intraperitoneal injection of 50 mg/kg pentobarbital sodium and then radiographs were taken with X-ray apparatus (Softex, Tokyo, Japan) and industrial X-ray film (Fuji Photo Film, Tokyo, Japan) that were operated at a voltage of 55 kV against 3.2 mA s^{-1} with a tube-to-film distance of 110 cm for lateral projection.

2.12. Histological analysis

Animals were humanely sacrificed *via* cervical dislocation on the 29th day, and right hind paws were excised for histopathological evaluation. The ankle joints removed from the hind paws were fixed for 24 h in 10% neutral buffered formalin(pH 7.2). After being dehydrated through a series of ethanol solutions, embedded in paraffin, tissue sections (2 ??m thick) were stained with hematoxylin and eosin (H&E) for

histopathological examination. A blinded and experienced pathologist evaluated the slides under light microscope and photographed the stained tissues.

2.13. Hematological assessment

On the 29th day, blood samples were withdrawn from each rat *via* cardiac puncture into test tubes containing anticoagulant (5% EDTA). Blood samples were then analyzed by a haem automated analyzer (Cell Dyne: Model 331430, Abbott Laboratories, IL, USA) for total blood count and specific white blood cells differentials.

2.14. Biochemical analysis of serum

Collected blood samples were allowed to clot for 30 minutes at room temperature and were centrifuged at 1000 rpm for 10 minutes. The sera obtained were stored at -20 °C until biochemical analysis was carried out. Serum indices were analyzed by an automated analyzer (ATAC 8000, Elan Diagnostics, CA, USA) and estimated for total protein, total bilirubin/direct and indirect bilirubin, aspartate aminotransferase (AST), creatinine (CRE), urea and blood urea nitrogen (BUN).

2.15. Statistical analysis

A sample size of five rats per group were used in the *in vivo* test. Mean ± standard error of mean (SEM) were used in presenting all data. One-way ANOVA with Tukey's*post hoc* test were used to determine differences between these treatment groups (areas under the curves). Graphpad® Prism Version 7.0 (Graphpad Software, San Diego, CA, USA)

for Windows was used to perform all statistical analysis. $P<0.05$ was considered statistically significant for all tests.

3. Results and discussion

3.1. Structural elucidation

Compound **1**, obtained as needle-like crystals, gave the molecular formula $C_{30}H_{50}O$ by the ^{13}CNMR data analysis (30 carbon signals) and from the HRMS sodium adduct ions at *m/z* 449.3800 $[M+Na]^+$ (calculated for $C_{30}H_{50}ONa$, 449.3759) and 875.7696 $[2M+Na]^+$ (calculated for $C_{60}H_{100}O_2Na$, 875.7621), corresponding to 6 indices of hydrogen deficiency. Its IR spectrum showed a characteristic broad absorption band at 3253 cm^{-1}, implying the presence of a hydroxy functionality. ^{13}CNMR signals at δ 145.35 and 121.89 suggested the existence of an olefinic motif. It could also be observed from the ^{1}HNMR spectrum of compound **1** that there were 8 methyl groups in this compound. These signals were at δ 0.79, 0.83, 0.94, 0.97, 1.00, and 1.14 (each 3H, s), and 0.87 (3H × 2, s). Additionally, there were one triplet peak at δ 5.18 (J = 3.56 Hz, 1H) and one *dd* peak at δ 3.22 (J_1= 10.84 Hz, J_2= 4.56 Hz, 1H) in the spectrum. In general, the NMR spectroscopic data of compound **1** were somewhat comparable to those of compound **2**, suggesting that they resemble each other.

Compound **2** was isolated as shiny crystals with a specific rotation of $[\alpha]^{24}_D$−38.45 (*c* 0.07, $CHCl_3$). The molecular formula of compound **2** was determined to be $C_{30}H_{48}O_3$ by the HRMS ions at *m/z* 479.3512 $[M+Na]^+$ (calculated for $C_{30}H_{48}O_3Na$, 479.3501) and 935.7116 $[2M+Na]^+$ (calculated for $C_{60}H_{96}O_6Na$, 935.7105) and from the ^{13}CNMR

spectrum which showed also 30 carbon signals (Table 1). The IR spectrum exhibited two separate bands at 3532 and 3435 $cm^{-1}$and a sharp band at 1663 cm^{-1}, together with a broad absorption band between 3300 and 2500 cm^{-1}, suggesting the presence of a carboxylic acid group with hydrogen bonding. A sharp absorption band at 1726 cm^{-1} seen in the IR spectrum indicated the presence of a ketone group. ^{13}CNMR signals at δ 184.12 and 213.21 confirmed the existence of these two functional groups. Molecular formula of compound **2** implied 7 indices of hydrogen deficiency. We then obtained the X-ray crystal structure of compound **2** (Fig. 1), which is in accord with its molecular formula. Crystallographic data and structural refinement parameters for compound **2** are given in Table 2, and geometric parameters are shown in Tables S1 and S2. The C-C distances of all five cyclohexane rings are within normal range of 1.52-1.57 Å. The carboxylic group makes strong hydrogen bond interactions with a water molecule, found in the crystal lattice. The water molecule also mediates hydrogen bond interactions with two symmetry-related molecules (O3-H3 … O4 (1.8449(1) Å, O4-H … $O2^{i}$ (1.9659(1) Å (symmetry code: 1/2-x, 1/2+y, 1-z) and O4-Ha … $O2^{ii}$ (2.0843(1) (symmetry code: +x, 1+y, +z)) leading to the formation of a stable polymeric structure along the b axis (Fig. S1). The hydrogen-bond geometry is shown in Table S3. Packing diagram of the crystal structure is shown in Fig. S2. Unlike the carboxylate, the oxygen atom of the carbonyl group is not involved in any hydrogen bond interaction.

Upon literature investigations, compound **2** was elucidated to be a known triterpene derivative, polpunonic acid (also maytenonic acid, or 3-oxofriedelan-29-oic acid). To the best of our knowledge, this is the first time that the absolute configuration of

polpunonic acid was determined by X-ray diffraction analysis[24-27]. The ^{1}HNMR assignments of the seven distinctive methyl groups for compound **2**were at δ 0.72, 0.86, 1.00, 1.10, and 1.26 (each 3H, s), and 0.88 (3H × 2, s), which were consistent with those reported in the literature [25].

With the defined structure of compound **2** in hand, we speculated that**1**should be a related triterpene-typed molecule (Fig. 2). Through comparison with spectroscopic data reported in the literature[28,29], compound **1** was finally identified as β-amyrin. The ^{13}CNMR assignments, which were generally consistent with reported values, were summarized in Table 1.

β-Amyrin, isolated together with α-amyrin (Fig. 2) as a mixture compound in certain cases, has been found in diverse plants and plant materials like bark, leaves, and resins[30-32]. Extensive studies have demonstrated that β-amyrin exhibits a variety of biological activities both *in vitro* and *in vivo,* such as antifungal[33], antibacterial[34], anti-inflammatory[29, 35-37], potential anticancer activities[38, 39], etc. Polpunonic acid was first isolated from *Maytenus senegalensis* (Celastraceae) and structurally elucidated by Abraham et.al in 1971[25]. From then on, a mass of research work on the isolation from different plants and broad bioactivities of this compound have been reported. It has been found that polpunonic acid shows antibacterial[40], anti-inflammatory[41,42], antinociceptive[43], cytotoxic activities[44], and so on.

The complete Freund's adjuvant (CFA)-induced arthritis in rats is a well-established animal model that mimics the human rheumatoid arthritis, comprising of joint swelling, loss of joint function, cartilage degradation and pain[45]. One of the most important

features of this model is chronic synovitis, which includes the infiltration of inflammatory cells and synovial hyperplasia[46].Therefore, CFA-induced arthritis in rats has been employed frequently to assess the possible medicinal effects of test agents in the treatment of RA [47].

As mentioned above, preliminary studies in our lab indicated that extracts of *Ziziphus abyssinica*'s root bark exhibited prominent anti-inflammatory activity in several *in vitro* and *in vivo* models of acute inflammation. We speculated *β*-amyrin and polpunonic acid could be possibly responsible for the anti-inflammatory activity of the extracts of *Ziziphus abyssinica*in these models. In fact, one previous study from Prof. Calixto's group revealed that oral administration with a dose of 30 mg/kg of *α,β*-amyrin (mixture of both compounds) significantly reduced inflammation induced by CFA in mice, through directly activating the cannabinoid receptors type 1/2(CB1 and CB2)[48]. With the very few *in vivo* anti-inflammatory studies that have been conducted on either compound so far, none of them looked at the compounds' effect on rheumatoid arthritis/chronic inflammation in the *in vivo* model, and none of these reports focused on *β*-amyrin (without *α*-amyrin) or polpunonic acid as a pure chemical entity. Therefore, there is a necessity to investigate the *in vivo* anti-inflammatory effects against chronic inflammation of *β*-amyrin (without *α*-amyrin) and polpunonic acid in the CFA-induced arthritis model in rats, identifying whether they are the anti-inflammatory compositions of this plant and further to enrich the biological activity study of these two triterpene-type compounds.

3.2. Anti-arthritic activity study in chronic immunological CFA-induced arthritis in rats

In this study, CFA was injected intraplantarly into the right hind paws of rats in all groups except non-arthritic control group on day 0. Arthritic control group received only intraplantar injection of CFA, whilst non-arthritic control group received only intraplantar injection of incomplete Freund's adjuvant (IFA) on day 0. Treatment groups received dexamethasone (3 mg/kg, *p.o.*), **1** (3, 10, 30 mg/kg, *p.o.*), **2** (3, 10, 30 mg/kg, *p.o.*) or distilled water (10 mL/kg) once every day from day 14 to day 28. All doses were constituted as an emulsion using Tween-80 (0.5% v/v). Anti-arthritic activities of compounds **1** and **2** were evaluated on body weights, hind paw thickness, arthritic score, and morphological changes of hind limbs. On day 29, blood samples were withdrawn *via* cardiac puncture for assessment of hematological parameters and animals were sacrificed *via* cervical dislocation to facilitate histopathologic examination of the joints.

*3.2.1.Effect of compounds **1** and **2** on total change in body weight*

In many disease states including rheumatoid arthritis, change in body weight is an important determinant of health [49, 50]. Since the rats were well-fed throughout the 28 days treatment period, it was expected that they would gain weight. As shown in Fig. 3 and Table S4, the total change in body weight (AUC) obtained by the IFA group was 171.50, while rats in the CFA-treated only group gained the least total change in body weight (AUC = 18.65). This could be due to the generation of immune responses associated with the disease [50]. As expected, the total changes in body weight of the

rats in all compound-treatment groups were significantly ($P < 0.05$) higher than that of the CFA-treated only group. Specifically, rats treated with compound **1** at 3, 10 and 30 mg/kg obtained total changes in body weight of 261.40, 272.60, and 368.70, respectively, whereas those rats treated with compound **2** at 3, 10 and 30 mg/kg obtained total changes in body weight of 98.24, 214.10, and 245.10, respectively. Furthermore, the total change in body weight of rats treated with compound **1** at 3 mg/kg (261.40) was also higher than that of rats treated with dexamethasone at 3 mg/kg (163.30), suggesting that a better therapeutic effect was achieved.

*3.2.2. Effect of compounds **1** and **2** on hind paw thickness*

CFA-induced arthritis is known to encompass both primary (acute) and secondary (polyarthritis) arthritic phases. In the primary phase, there is pronounced swelling of the ipsilateral paw, which is mediated by prostaglandins[51]. This is followed by an inflammation in the contralateral paws (secondary phase) in which auto-antibodies are generated[52]. An effective anti-arthritic agent should be able to suppress one or both of these phases. Therefore, the measurement of paw thickness has been widely employed as an assessment tool for anti-arthritic agents [50].

Treatment with **1** (3, 10, and 30 mg/kg), **2** (3, 10, and 30 mg/kg), or dexamethasone (3 mg/kg) started on day 14 following the onset of the secondary phase of the chronic inflammation. The time dependent changes in the hind paw thickness of rats were presented in Fig. 4 and Table S4. Progressive increase in the contralateral (non-injected) paw thickness was seen in all CFA administered groups from day 12. This was

indicative of systemic spread of the inflammation. Compounds **1** and **2** at all doses significantly ($P<0.05$) altered the time course of edema progression of the arthritis. As such, there were remarkable decreases in the total change in paw thickness in both ipsilateral and contralateral paws of these arthritic rats by treatment of compounds **1** and **2** compared to those of CFA-treated only group. This decrease in paw swelling has been ascribed as an anti-arthritic effect of both compounds **1** and **2**.

*3.2.3. Effect of compounds **1** and **2** on arthritic score*

Adjuvant-induced arthritis is known to be associated with release of a number of inflammatory mediators (prostaglandins, lipoxygenases, etc.) which are responsible for the swelling, pain, destruction of bone and cartilage resulting in a severe disability and an increased arthritis score [53]. As shown in Fig. 5 and Table S4, the administration of CFA into the paws of the rats resulted in a very high arthritic score (14.25) and this was significantly ($P < 0.001$) reduced by treatment of compound **1** (30 mg/kg) to 6.5, as well as by treatment of compound **2** (10 mg/kg and 30 mg/kg) to 9.5 and 6.5, respectively. These ameliorative effect were comparable to that of the reference drug dexamethasone (3 mg/kg) which also significantly ($P < 0.001$) reduced the arthritic score to 6.5.

*3.2.4. Effect of compounds **1** and **2** on morphological changes of hind limbs*

As clearly shown in Fig. 6, there were no signs of erythema and edema in the rats of the non-arthritic (IFA) group (Fig. 6A). Rats in arthritic (CFA) control group (Fig. 6B),

however, exhibited massive erythema and swelling in both ipsilateral and contralateral hind limbs. The oral administration of dexamethasone (3 mg/kg, Figure 6C) caused a reduction in swelling in both ipsilateral and contralateral limbs. Treatment with different doses of compounds **1** (Fig. 6D-F) and **2** (Fig. 6G-I) resulted in reduced erythema and swelling with the effect of 30 mg/kg dose of both compounds comparable to that of dexamethasone (3 mg/kg). The morphological changes in the hind limbs as described in this section corresponds to the arthritic score described under section *3.2.3.*

*3.2.5. Effect of compounds **1** and **2** on lesions and joint deformation*

Radiograph presented in Fig. 7A showed that no lesions and joint deformation were detected in the non-arthritic (IFA) control group as expected. In contrast, the arthritic (CFA) control group, displayed noticeable signs of inflammation in both the ipsilateral and contralateral hind limbs including the tissues surrounding the bones of the foot. There were also noticeable signs of inflammation at the metatarsal-phalangeal joints. Bone enlargement with active osteophytosis was characterized by very thin trabecula extending from bone to connective tissue. The osteophytosis was marked on bone metaphysis and linked with lacunae. There were no observable joint spaces, and some bone islets arose in the connective tissue which was thickened and significantly enlarged. Eroding of the phalangeal bone was also observed. Treatment with the highest dose of both **1** and **2**, as well as dexamethasone (3 mg/kg) resulted in the prevention of inflammation and subsequently reduced the development of arthritic joint. Therefore, inflammation did not significantly spread to the affected connective tissues and bones.

In the low and medium doses of **1** and **2**, there were mild signs of inflammation and osteophytosis compared with the CFA control group.

*3.2.6. Effect of compounds **1** and **2** on histopathology*

Fig. 8 shows histopathological examination under a light microscope (×100) of rat joints where the articular cartilage was stained with haematoxylin and eosin (H&E). The disease severity and the effect of test compounds on articular cartilage histology were illustrated by photomicrographs. The pathological features, including cartilage erosion (white arrow), subchondral cyst (yellow arrow) and Weichselbaum's lacunae (red arrow),were observable in each experimental group. Therefore, the assessment of positive therapeutic effect was based on the degree and/or number of pathological features present in each group.

The IFA control group (Fig.8A) demonstrated an intact articular cartilage with no signs of cartilage erosion and Weichselbaum's lacunae, and no sign of pannus invasion leading to the formation of subchondral cyst. In contrast, the CFA control group (Fig.8B)exhibited all the three pathological features. The dexamethasone treatment group (Fig.8C) showed no signs of subchondral cyst and Weichselbaum's lacunae as there was an extensive erosion and thus loss of articular cartilage. The compounds **1** and **2** treatment groups displayed a reduction in these features. The group treated with 3 mg/kg of compound **1** (Fig.8D) showed high resolution of pannus invasion, fewer Weichselbaum's lacunaes with less articular erosion compared to the other treatment

groups. Subchondral cysts formed in group treated with 10 mg/kg of compound **2** (Fig.8H) were relatively larger but less than that of the CFA control group. Increased Weichselbaum's lacunae was observed in groups treated with **1** (30 mg/kg, Fig. 8F), **2** (10 mg/kg, Fig. 8H), and **2** (30 mg/kg, Fig. 8I) compared to the other treatment groups, but relatively less than that of the CFA control group.

Histopathological examination under a light microscope (×100) of rat joints where the articular bone structure was stained with H&E is depicted in Fig. 9. Histological features with evidence of bone remodeling and tissue infiltration of mononuclear inflammatory cells were assessed. The IFA control group (Fig. 9A) exhibited an intact architecture of bone structure, no evidence of osteoclast activity and infiltration. In contrast, the CFA control group (Fig. 9B) showed extensive inflammation, blood vessel congestion with increased infiltration of mononuclear inflammatory cells. The results of the histological analysis indicated that inflammation as well as bone structure destruction were significantly reduced after treatment with dexamethasone (Fig. 9C). There were evidences of bone remodeling and reduced bone cavitation in all groups treated with compounds **1** and **2**compared to the CFA control group. The most improved tissue architecture was observed in the group treated with 3 mg/kg of compound **1** (Fig. 9D) compared to other treatment groups. The order of amelioration of bone destruction is as follows: compound **1 (**3 mg/kg) > **2** (30 mg/kg) > **2** (3 mg/kg) >**1** (30 mg/kg) >**2** (10 mg/kg).

*3.2.7. Effect of compounds **1** and **2** on hematological parameters*

Data presented in Fig. 10, Fig. 11, and Table S5 shows that there was no significant difference between IFA- and CFA-treated (with or without drug treatment) rats with respect to most of the hematological parameters assessed. However, the white blood cell (WBC) count of CFA-treated only rats ($15.47\times10^3/mm^3$) was significantly ($P<0.01$) higher than those of the IFA-treated group of rats ($2.33\times10^3/mm^3$). This increase in WBC count has been suggested to be an immune reaction in response to the stimulation of the immune system against the invading antigens from the CFA [54]. As expected, compared to the CFA-treated only group, there was a significant ($P < 0.05$) decrease in WBC count by the treatment of compound **1** at 3, 10 and 30 mg/kg to $10.75\times10^3/mm^3$, $10.36\times10^3/mm^3$, and $8.61\times10^3/mm^3$, respectively. Similarly, treatment of compound **2** at 3, 10 and 30 mg/kg also displayed a significant ($P < 0.05$) immunomodulatory effect by decreasing WBC count to $7.09\times10^3/mm^3$, $7.20\times10^3/mm^3$, and $4.58\times10^3/mm^3$, respectively. In addition, this increase in WBC count of the rats by treatment of CFA was significantly ($P<0.05$) reduced following treatment of dexamethasone (3 mg/kg, $5.83\times10^3/mm^3$).

It has been observed that anemic condition characterized by a decrease in the red blood cell (RBC) count and hemoglobin levels usually appears to be the most common extraarticular manifestation of rheumatoid arthritis [55]. In the present study, there were reductions in the RBC count, hemoglobin and hematocrit concentrations in the CFA-treated only group ($7.98\times10^6/mm^3$, 12.10 g/dL, and 34.93%, respectively) of rats compared with those of the IFA treatment group ($9.88\times10^6/mm^3$, 16.60 g/dL, and

48.35%, respectively), though not statistically significant (P>0.05). The RBC count in groups which were treated with compound **1** at 10 and 30 mg/kg increased slightly (8.71×10^6/mm^3 and 9.02×10^6/mm^3, respectively) compared to that of the CFA-treated only group, while the rest of the treatments did not.

*3.2.8. Effect of compounds **1** and **2** on serum biochemistry*

The assessment of serum biochemical parameters such as total protein, total bilirubin, AST, CRE, BUN/CRE ratio is an important tool for evaluating the anti-arthritic activity of a particular test agent. Obviously, these parameters were not significantly affected by either CFA alone or in combination with subsequent treatment with dexamethasone, **1** or **2**. However, the levels of total/indirect bilirubin and CRE were all elevated in the CFA control group, though not statistically significant. In addition, the level of BUN increased a little after treatment with compound **1** at 3, 10, and 30 mg/kg doses when compared with that of CFA control group. In general, both compounds **1** and **2** did not markedly impact on these serum biochemical parameters (Fig. 12 and Table S6).

4. Conclusions

In summary, we have isolated compounds **1** and **2** from the root bark of *Ziziphus abyssinica* and elucidated them as *β*-amyrin and polpunonic acid, respectively. Comprehensive work have been done on the isolation from diverse plants and bioactivity studies of both compounds before, and they displayed various biological

activities, such as antibacterial, anti-inflammatory, and cytotoxicity activities, etc. Additionally, our preliminary study revealed that extracts of the root bark of *Ziziphus abyssinica* exhibited prominent anti-inflammatory activity against acute inflammation. We therefore speculated it's possible that *β*-amyrin and polpunonic acid could be responsible for the anti-inflammatory activity of the extracts of the root barkof *Ziziphus abyssinica*.

Up to now, there hasn't been any study performed on *β*-amyrin and polpunonic acid to test their activities against chronic inflammationin the well-established CFA-induced arthritis model. Naturally, the two triterpene-type compounds were further evaluated for their *in vivo* anti-arthritic activity through the CFA-induced arthritis model in rats. Compared to those of the arthritic control group, treatment with **1** or **2** at 3, 10, and 30 mg/kg doses significantly reduced the primary, as well as the secondary paw swelling and the arthritis score in the later stage of adjuvant induced arthritis. Both compounds markedly reversed cartilage erosion, subchondral cyst, and Weichselbaum's lacunae formation through histopathological examinations of the hind paws of the rats. In addition, evidence of bone remodeling was observed in all groups of rats treated with **1** or **2**. Moreover, treatment with **1** or **2** at the various doses did not have significant impact on common hematological parameters and serum biochemical parameters. We therefore believe that *β*-amyrin and polpunonic acid are promising anti-arthritic agents. Studies on the mechanism of action of these two compounds are ongoing in our lab and this will be reported in due course.

Conflict of interest

The authors declare no competing financial interest.

Acknowledgements

This work was partially supported by NIH/NIDADA024022 (Y.Z.), NIH/NIMHD grant MD009124 (M.K.S.). Structural biology resources were provided by NIH Shared Instrumentation Grant S10-OD021756 (M.K.S.) and Virginia General Assembly Higher Education Equipment Trust Fund (HEETF) to Virginia Commonwealth University.

Appendix A. Supplementary material

Supplementary data to this article can be found online at.

References

[1] Q. Guo, Y. Wang, D. Xu, J. Nossent, N.J. Pavlos, J. Xu, Rheumatoid arthritis: pathological mechanisms and modern pharmacologic therapies, Bone Res., 6 (2018) 15.

[2] A. Jabeen, M.A. Mesaik, S.U. Simjee, Lubna, S. Bano, S. Faizi, Anti-TNF-α and anti-arthritic effect of patuletin: A rare flavonoid from Tagetes patula, Int. Immunopharmacol., 36 (2016) 232-240.

[3] D.G. Palmer, The anatomy of the rheumatoid lesion, Br. Med. Bull., 51 (1995) 286-295.

[4] V.H. Begum, J. Sadique, Long term effect of herbal drug Withania somnifera on adjuvant induced arthritis in rats, Indian J. Exp. Biol., 26 (1988) 877-882.

[5] R. Rajendran, E. Krishnakumar, Anti-arthritic activity of Premna serratifolia Linn., wood against adjuvant induced arthritis, Avicenna J. Med. Biotechnol., 2 (2010) 101-106.

[6] S. Singh, V. Nair, Y.K. Gupta, Antiarthritic activity of Majoon Suranjan (a polyherbal Unani formulation) in rat, Indian J. Med. Res., 134 (2011) 384-388.

[7] W.A. Kaleem, N. Muhammad, H. Khan, A. Rauf, Pharmacological and phytochemical studies of Genus Zizyphus, Middle-East J. Sci. Res. 21 (2014) 1243-1263.

[8] C. Orwa, A. Mutua, R. Kindt, R. Jamnadass, A. Simons, Agroforestree database: a tree species reference and selection guide version 4.0, World Agroforestry Centre ICRAF, Nairobi, KE, 2009.

[9] M.O. Nyaberi, C.A. Onyango, F.M. Mathooko, J.M. Maina, M. Makobe, F. Mwaura, Evaluation of phytochemical, antioxidant and antibacterial activity of edible fruit extracts of Ziziphus abyssinica A. Rich, J. Anim. Plant Sci., 6 (2010) 623-629.

[10] C.G. Wagate, J.M. Mbaria, D.W. Gakuya, et al., Screening of some Kenyan medicinal plants for antibacterial activity, Phytother. Res., 24 (2010) 150-153.

[11] M. Gundidza, M. Sibanda, Antimicrobial activities of ziziphus abyssinica and berchemia discolor, Cent. Afr. J. Med., 37 (1991) 80-83.

[12] C.N. Muthaura, J.M. Keriko, C. Mutai, et al., Antiplasmodial potential of traditional phytotherapy of some remedies used in treatment of malaria in Meru-Tharaka Nithi County of Kenya, J. Ethnopharmacol., 175 (2015) 315-323.

[13] M.O. Ugwah, E.U. Etuk, S.O. Bello, A.A. Aliero, C.J. Ugwah-Oguejiofor,

Comparative studies of anti-ulcerogenic activities of three Nigerian medicinal plants: A preliminary evaluation, J. Med. Plant. Res., 7 (2013) 490-495.

[14] C.J. Ugwah-Oguejiofor, Y.I. Alkali, O.M. Ugwah, K. Abubakar, Anti-diarrhoeal potential of the aqueous root extract of Ziziphus abyssinica A. Rich, Sch. Acad. J. Pharm., 2(2013) 419-423.

[15] E. Boakye-Gyasi, I.T. Henneh, W.K.M. Abotsi, E.O. Ameyaw, E. Woode, Hydro-ethanolic leaf extract of Ziziphus abyssinica Hochst Ex A. Rich (Rhamnaceae) exhibits anti-nociceptive effects in murine models, BMC Complement. Altern. Med., 17 (2017) 231.

[16] E. Boakye-Gyasi, I.T. Henneh, W.K.M. Abotsi, E.O. Ameyaw, E. Woode, Possible mechanisms involved in the anti-nociceptive effects of hydro-ethanolic leaf extract of Ziziphus abyssinica, Pharm. Biol., 55 (2017) 1962-1971.

[17] I.T. Henneh, E.O. Ameyaw, R.P. Biney, et al., Ziziphus abyssinica hydro-ethanolic root bark extract attenuates acute inflammation possibly through membrane stabilization and inhibition of protein denaturation and neutrophil degranulation, West African J. Pharm., 29 (2018) 81-94.

[18] O.D. Rigaku, CrysAlis PRO, Rigaku Oxford Diffraction Ltd. Yarnton, Oxfordshire, England, 2015.

[19] G.M. Sheldrick, SHELXT-Inyegrated space-group and crystal-structure determination, Acta Crystallogr. A Found. Adv., A71 (2015) 3-8.

[20] L.J. Bourhis, O.V. Dolomanov, R.J. Gildea, J.A.K. Howard, H. Puschmann, The anatomy of a comprehensive constrained restrained refinement program for the modern

computing environment-Olex2 dissected, Acta Crystallogr. A Found. Adv., A71 (2015) 59-75.

[21] O.V. Dolomanov, L.J. Bourhis, R.J. Gildea, J.A.K. Howard, H. Puschmann, OLEX2: a complete structure solution, refinement and analysis program, J. Appl. Cryst., 42 (2009) 339-341.

[22] C.M. Pearson, F.D. Wood, Studies of polyarthritis and other lesions induced in rats by injection of mycobacterial adjuvant. I. General clinical and pathologic characteristics and some modifying factors, Arthritis Rheum., 2 (1959) 440-459.

[23] J. Paval, S.K. Kaitheri, B.K. Potu, et al., Anti-arthritic potential of the plant Justicia gendarussa Burm F, Clinics (Sao Paulo), 64 (2009) 357-362.

[24] H. Itokawa, O. Shirota, H. Ikuta, H. Morita, K. Takeya, Y. Iitaka, Triterpenes from Maytenus ilicifolia, Phytochemistry, 30 (1991) 3713-3716.

[25] D.J. Abraham, J. Trojánek, H.P. Münzing, H.H.S. Fong, N. R. Farnsworth, Structure Elucidation of Maytenonic Acid, a New Triterpene from Maytenus Senegalensis (Celastraceae), J. Pharm. Sci., 60 (1971) 1085-1087.

[26] H. Nozaki, Y. Matsuura, S. Hirono, R. Kasai, J.-J. Chang, K.-H. Lee, Antitumor Agents, 116. Cytotoxic Triterpenes from Maytenus diversifolia, J. Nat. Prod., 53 (1990) 1039-1041.

[27] C.H. Lu, J.X. Zhang, F.Y. Gan, Y.M. Shen, Chemical constituents of the suspension cell cultures of Maytenus hookeri, Acta Botanica Sinica, 44 (2002) 603-610.

[28] U.V. Mallavadhani, A. Mahapatra, K. Jamil, P.S. Reddy, Antimicrobial activity of

some pentacyclic triterpenes and their synthesized 3-O-lipophilic chains, Biol. Pharm. Bull., 27 (2004) 1576-1579.

[29] N.N. Okoye, D.L. Ajaghaku, H.N. Okeke, E.E. Ilodigwe, C.S. Nworu, F.B.C. Okoye, beta-Amyrin and alpha-amyrin acetate isolated from the stem bark of Alstonia boonei display profound anti-inflammatory activity, Pharm. Biol., 52 (2014) 1478-1486.

[30] F.A. Oliveira, C.L.S. Costa, M.H. Chaves, et al., Attenuation of capsaicin-induced acute and visceral nociceptive pain by α- and β-amyrin, a triterpene mixture isolated from Protium heptaphyllum resin in mice, Life Sci., 77 (2005) 2942-2952.

[31] M.F. Otuki, J. Ferreira, F.V. Lima, et al., Antinociceptive Properties of Mixture of α-Amyrin and β-Amyrin Triterpenes: Evidence for Participation of Protein Kinase C and Protein Kinase A Pathways, J. Pharmacol. Exp. Ther., 313 (2005) 310-318.

[32] F.A. Oliveira, M.H. Chaves, F.R.C. Almeida, et al., Protective effect of α- and β-amyrin, a triterpene mixture from Protium heptaphyllum (Aubl.) March. trunk wood resin, against acetaminophen-induced liver injury in mice, J. Ethnopharmacol., 98 (2005) 103-108.

[33] K. Jabeen, A. Javaid, E. Ahmad, M. Athar, Antifungal compounds from Melia azedarach leaves for management of Ascochyta rabiei, the cause of chickpea blight, Nat. Prod. Res., 25 (2011) 264-276.

[34] J.F. Rivero-Cruz, S. Sánchez-Nieto, G. Benítez, et al., Antibacterial compounds isolated from Byrsonima crassifolia, Revista Latinoamericana de Química, 37 (2009) 155-163.

[35] S. A. Holanda Pinto, L. M. Pinto, G. M. Cunha, M. H. Chaves, F. A. Santos, V. S. Rao, Anti-inflammatory effect of alpha, beta-Amyrin, a pentacyclic triterpene from Protium heptaphyllum in rat model of acute periodontitis, Inflammopharmacology, 16 (2008) 48-52.

[36] C.E. Vitor, C.P. Figueiredo, D.B. Hara, A.F. Bento, T.L. Mazzuco, J.B. Calixto, Therapeutic action and underlying mechanisms of a combination of two pentacyclic triterpenes, α- and β-amyrin, in a mouse model of colitis, Br. J. Pharmacol., 157 (2009) 1034-1044.

[37] V.R. Askari, N. Fereydouni, V. Baradaran Rahimi, et al., β-Amyrin, the cannabinoid receptors agonist, abrogates mice brain microglial cells inflammation induced by lipopolysaccharide/interferon-γ and regulates Mφ1/Mφ2 balances, Biomed. Pharmacother., 101 (2018) 438-446.

[38] T. Mishra, R.K. Arya, S. Meena, et al., Isolation, Characterization and Anticancer Potential of Cytotoxic Triterpenes from Betula utilis Bark, PLoS One, 11 (2016) e0159430.

[39] K.M. de Melo, F.T.B. de Oliveira, R.A. Costa Silva, et al., α, β-Amyrin, a pentacyclic triterpenoid from Protium heptaphyllum suppresses adipocyte differentiation accompanied by down regulation of PPARγ and C/EBPα in 3T3-L1 cells. Biomed. Pharmacother., 109 (2019) 1860-1866.

[40] K.L. Lindsey, M. Budesinsky, L. Kohout, J. van Staden, Antibacterial activity of maytenonic acid isolated from the root-bark of Maytenus senegalensis, S. Afr. J. Bot., 72 (2006) 473-477.

[41] S. Sosa, C.F. Morelli, A. Tubaro, P. Cairoli, G. Speranza, P. Manitto, Anti-inflammatory activity of Maytenus senegalensis root extracts and of maytenoic acid, Phytomedicine, 14 (2007) 109-114.

[42] A. Villar-Lorenzo, A.E. Ardiles, A.I. Arroba, et al., Friedelane-type triterpenoids as selective anti-inflammatory agents by regulation of differential signaling pathways in LPS-stimulated macrophages, Toxicol. Appl. Pharmacol., 313 (2016) 57-67.

[43] S.F. Andrade, L.G.V. Cardoso, J.C.T. Carvalho, J.K. Bastos, Anti-inflammatory and antinociceptive activities of extract, fractions and populnoic acid from bark wood of Austroplenckia populnea, J. Ethnopharmacol., 109 (2007) 464-471.

[44] D. Fan, S. Parhira, G.Y. Zhu, Z.H. Jiang, L.P. Bai, Triterpenoids from the stems of Tripterygium regelii, Fitoterapia, 113 (2016) 69-73.

[45] X.F. Shen, Y. Zeng, J.C. Li, C. Tang, Y. Zhang, X.L. Meng, The anti-arthritic activity of total glycosides from Pterocephalus hookeri, a traditional Tibetan herbal medicine, Pharm. Biol., 55 (2017) 560-570.

[46] S. Ashraf, P.I. Mapp, D.A. Walsh, Angiogenesis and the persistence of inflammation in a rat model of proliferative synovitis, Arthritis Rheum., 62 (2010) 1890-1898.

[47] D.L. Asquith, A.M. Miller, I.B. McInnes, F.Y. Liew, Animal models of rheumatoid arthritis. Eur. J. Immunol., 39 (2009) 2040-2044.

[48] K.A. da Silva, A.F. Paszcuk, G.F. Passos, et al., Activation of cannabinoid receptors by the pentacyclic triterpene alpha,beta-amyrin inhibits inflammatory and neuropathic persistent pain in mice, Pain, 152 (2011) 1872-1887.

[49]E. M. Glenn, J. Gray, and W. Kooyers, Chemical changes in adjuvant induced polyarthritis of rats, Am. J. Vet. Res, 26(1965) 1195-1203.

[50] D. Nguemnang, S. Flore, E.G. Tsafack, et al., In Vitro Anti-Inflammatory and In Vivo Antiarthritic Activities of Aqueous and Ethanolic Extracts of Dissotis thollonii Cogn.(Melastomataceae) in Rats, Evid. Based Complement. Alternat. Med. 2019 (2019) 1-17.

[51]M. Choudhary, V. Kumar, P. Gupta, S. Singh, Investigation of antiarthritic potential of Plumeria alba L. leaves in acute and chronic models of arthritis, BioMed Res. Int., 2014 (2014) 1-12

[52]M.V.K. Patil, A.D. Kandhare, S.D. Bhise, Anti-arthritic and anti-inflammatory activity of Xanthium srtumarium L. ethanolic extract in Freund's complete adjuvant induced arthritis, Biomedicine &Aging Pathology, 2 (2012) 6-15.

[53] B. Lin, Y. Zhao, P. Han, et al, Anti-arthritic activity of Xanthium strumarium L. extract on complete Freund′ s adjuvant induced arthritis in rats, J Ethnopharmacol, 155(2014) 248-255.

[54] C. Rajaram, R. K. Ravindra, C. S. K. Bonnth, Evaluation of antiarthritic activity of Caesalpinia pulcherimma in Freund's complete adjuvant induced arthritic rat model, J. Young Pharmacists, 7(2015) 128-132.

[55] A. G. Mowat, Hematologic abnormalities in rheumatoid arthritis, Semin. Arthritis Rheum, 1(1971) 195-219.

Figure captions

Fig.1. X-ray crystal structure of compound **2**.

Fig.2. Chemical structures of compounds **1**, **2** and *α*-amyrin.

Fig. 3. Effect of **1** (a) and **2** (b) administration on the body weights of Sprague-Dawley rats.

Fig. 4. Effect of **1** and **2** administration on CFA-induced arthritis in Sprague-Dawley rats.

Fig. 5. Effect of **1** and **2** administration on the arthritic score determined on the 29th day of CFA -induced arthritis in Sprague-Dawley rats.

Fig. 6. Photographs showing the curative effect of **1** and **2** in CFA-induced arthritis in Sprague-Dawley rats.

Fig. 7. Radiographs showing the curative effect of **1** and **2** in CFA-induced arthritis in Sprague-Dawley rats.

Fig. 8. Histopathological examination of rat joints showing the articular cartilage stained with hematoxylin and eosin under a light microscope (× 100) in CFA-induced arthritis in Sprague-Dawley rats.

Fig. 9. Histopathological examination of rat joints showing the articular bone structure stained with hematoxylin and eosin under a light microscope (× 100) in CFA-induced arthritis in Sprague-Dawley rats.

Fig. 10. Effect of dexamethasone, **1** and **2** administration on the hematological parameters in CFA-induced arthritis in Sprague-Dawley rats.

Fig. 11. Effect of dexamethasone, **1** and **2** administration on the hematological

parameters in CFA-induced arthritis in Sprague-Dawley rats.

Fig. 12. Effect of dexamethasone, **1** and **2** administration on the

serum biochemical parameters in CFA-induced arthritis in Sprague-Dawley rats.

Figures

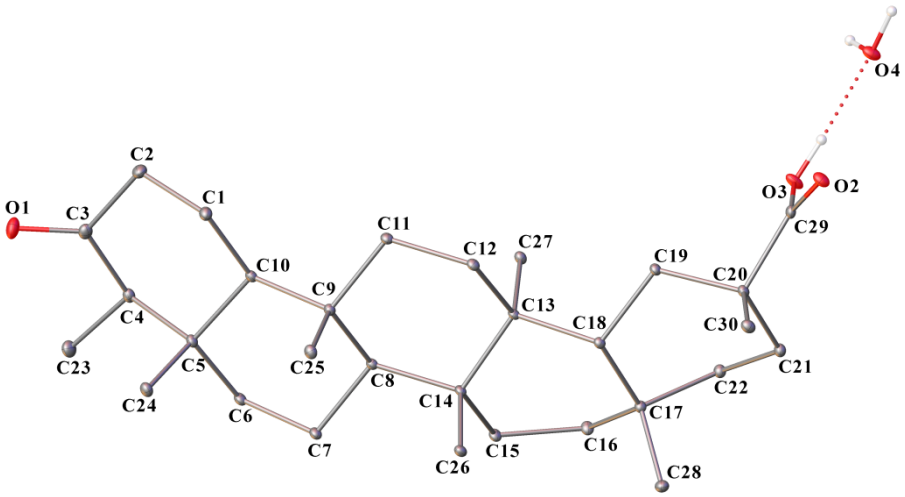

Fig.1. X-ray crystal structure of compound **2**.

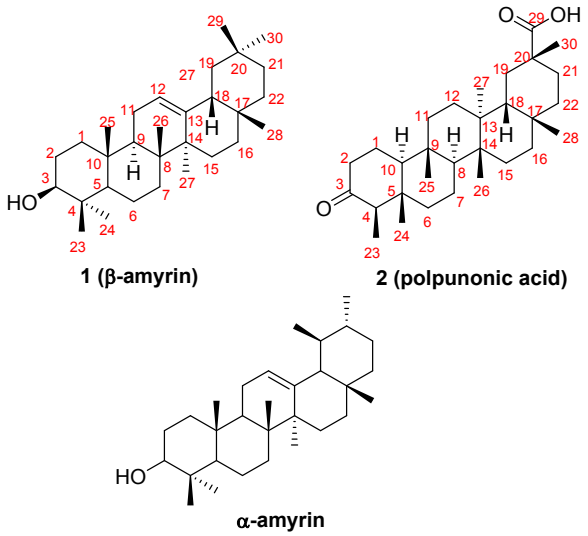

Fig.2. Chemical structures of compounds **1**, **2**and*α*-amyrin.

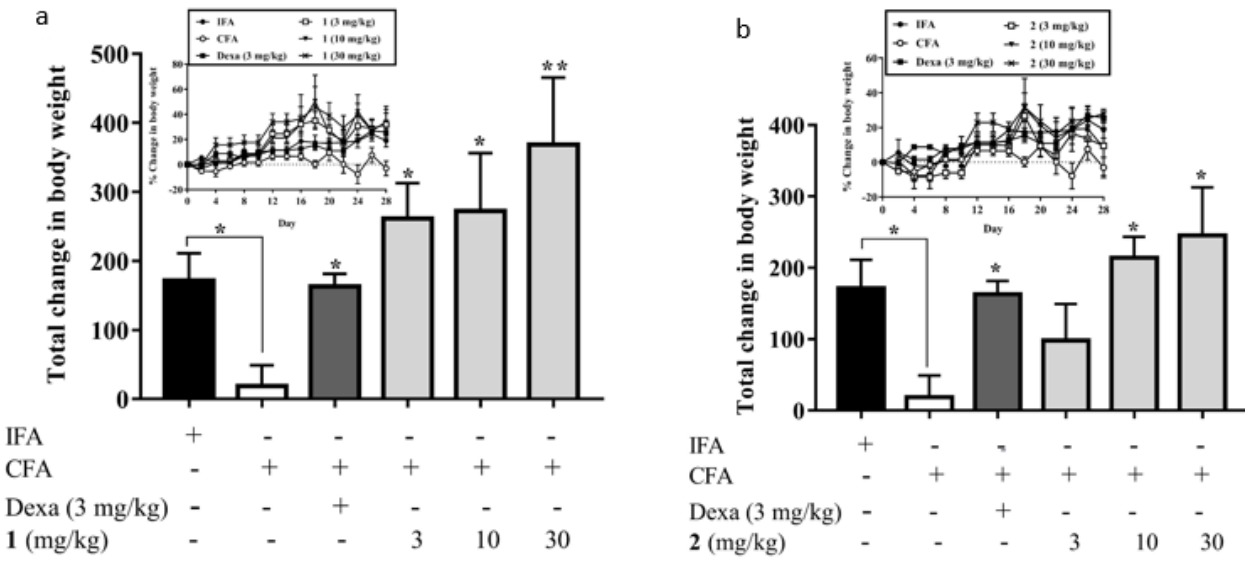

Fig. 3. Effect of **1** (a) and **2** (b) administration on the body weights of Sprague-Dawley rats. Data was represented as Mean ± SEM (n = 5). The total changes in body weight of the treatment groups were compared to that of the arthritic control group (CFA) with *P<0.05, **P<0.01(One-way ANOVA followed by Tukey's post *hoc* test). Insert: Time course curves of the percentage change in body weight of different treatments.

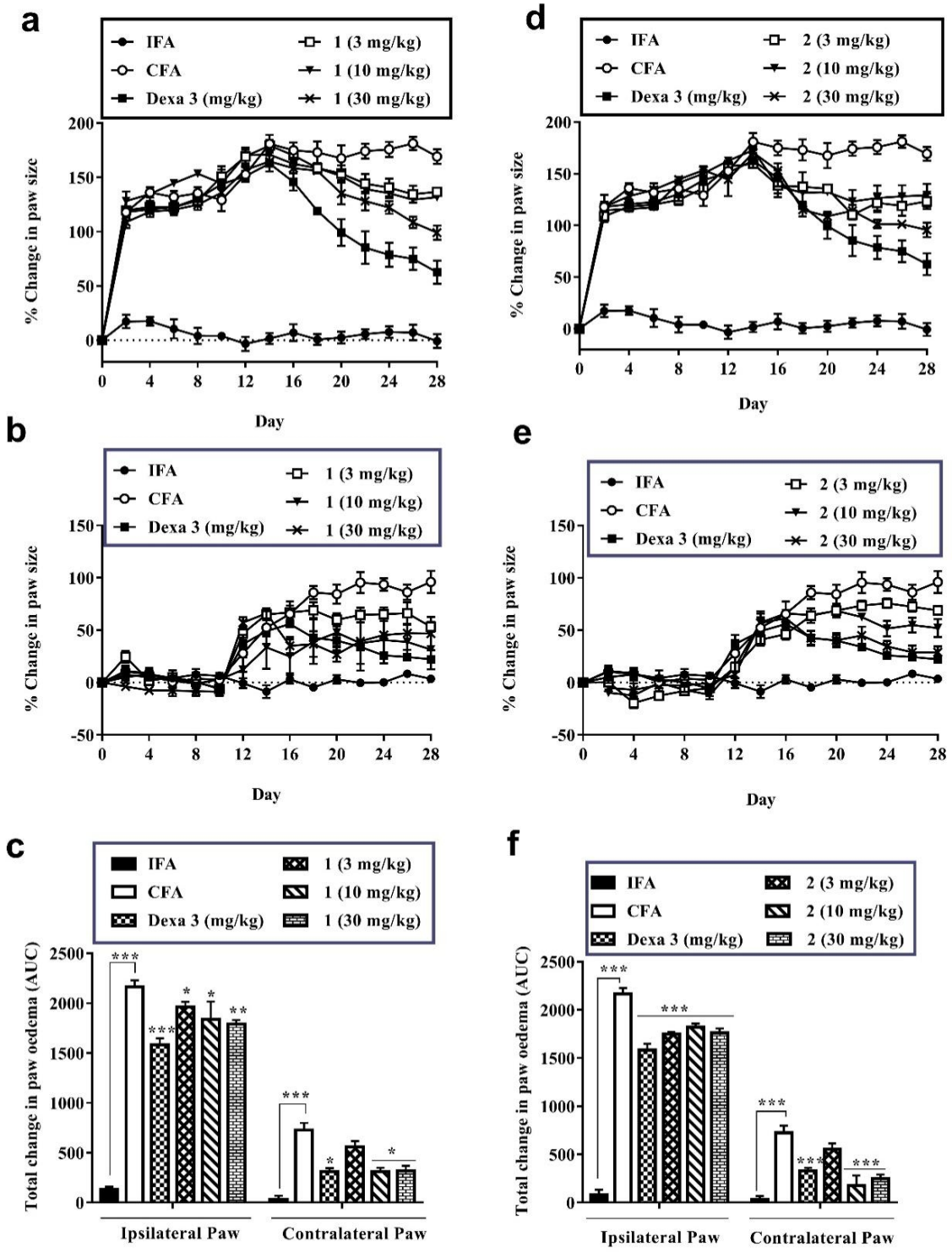

Fig. 4. Effect of **1** and **2** administration on CFA-induced arthritis in Sprague-Dawley rats. The edema component of inflammation was monitored as the percentage change in ipsilateral (a and b) and contralateral (d and e) pawedema for **1** and **2** respectively. Total edema induced during the acute and polyarthritis phases was calculated as area

under the time course curves, AUC (c and f). Data are presented as Mean ± SEM (n = 5). The total anti-edematous effect of treatment groups werecompared to that of the arthritic control group with *P < 0.05, **P <0.01, ***P <0.001 (One-way ANOVA followed by Tukey's post *hoc* test).

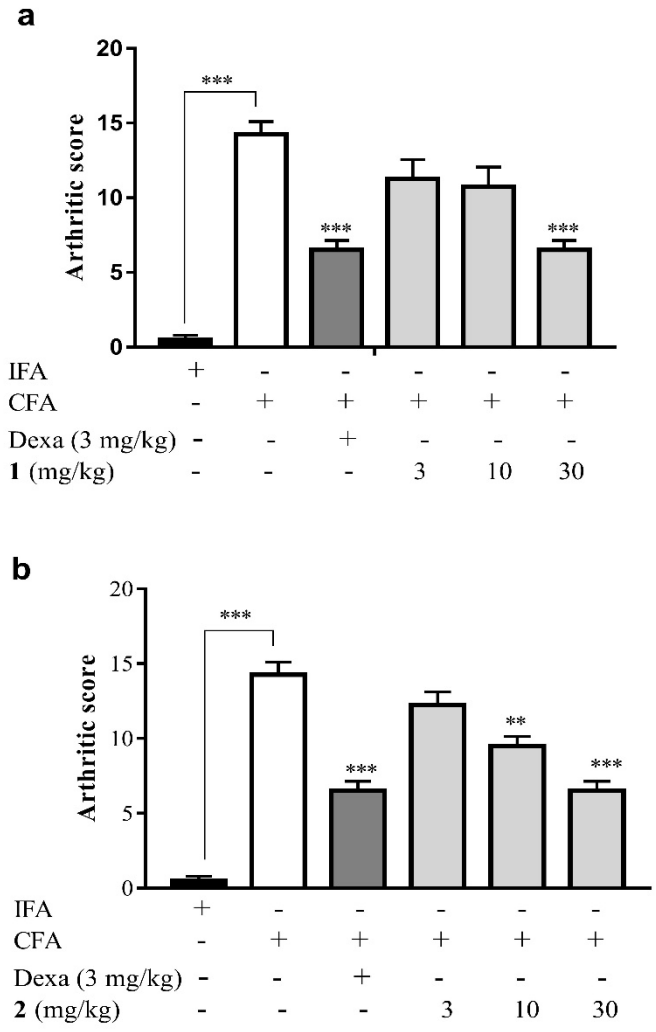

Fig. 5. Effect of **1** and **2** administration on the arthritic score determined on the 29th day of CFA -induced arthritis in Sprague-Dawley rats. Data are presented as Mean ± SEM (n = 5). The total anti-edematous effects of treatment groups were compared to

CFA control group with *P<0.05, **P <0.01, ***P <0.001 (One-way ANOVA followed by Tukey's post *hoc* test).

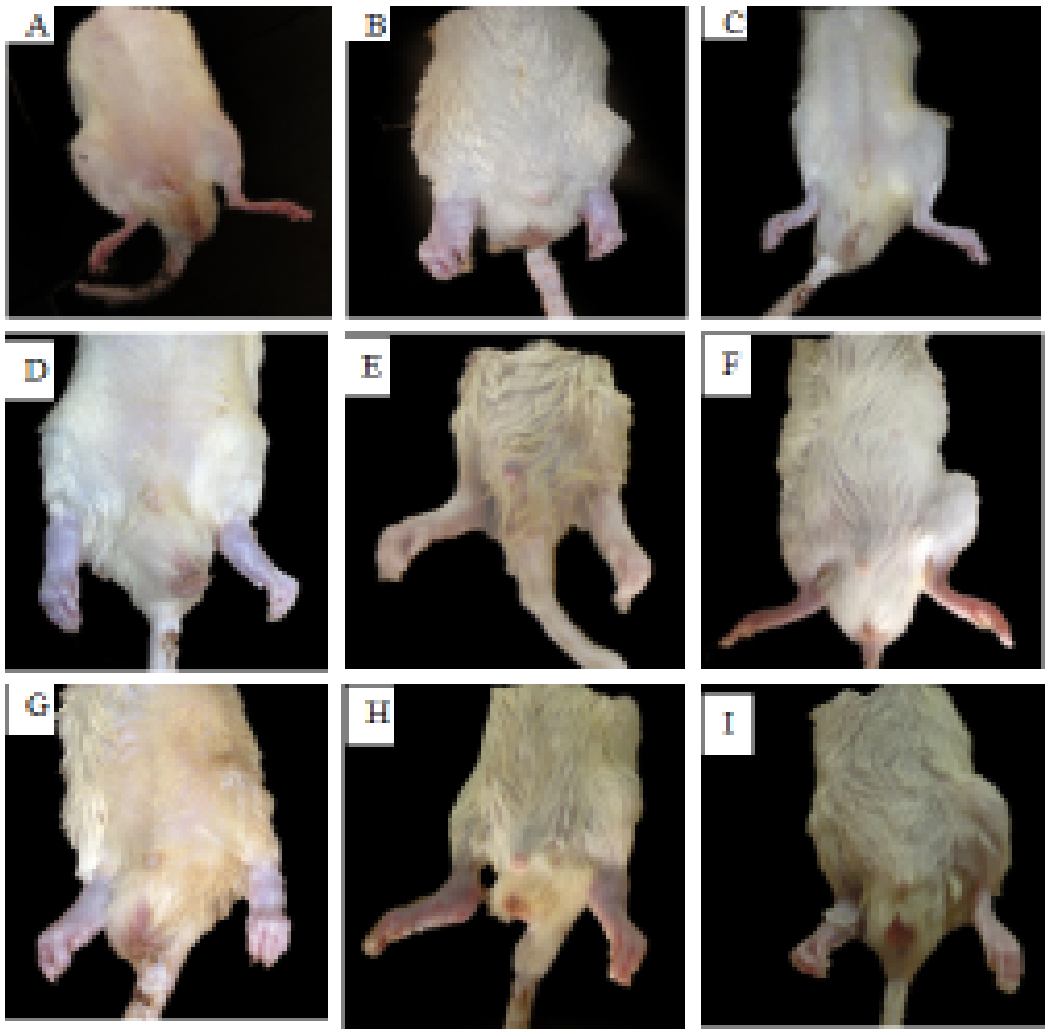

Fig. 6. Photographs showing the curative effect of **1** and **2** in CFA-induced arthritis inSprague-Dawley rats. (A)IFA/non-arthritic control, (B)CFA/arthritic control, (C) dexamethasone (3 mg/kg), (D) **1** (3 mg/kg), (E)**1** (10 mg/kg), (F)**1** (30 mg/kg), (G)**2** (3 mg/kg), (H)**2** (10 mg/kg), and (I)**2** (30 mg/kg).

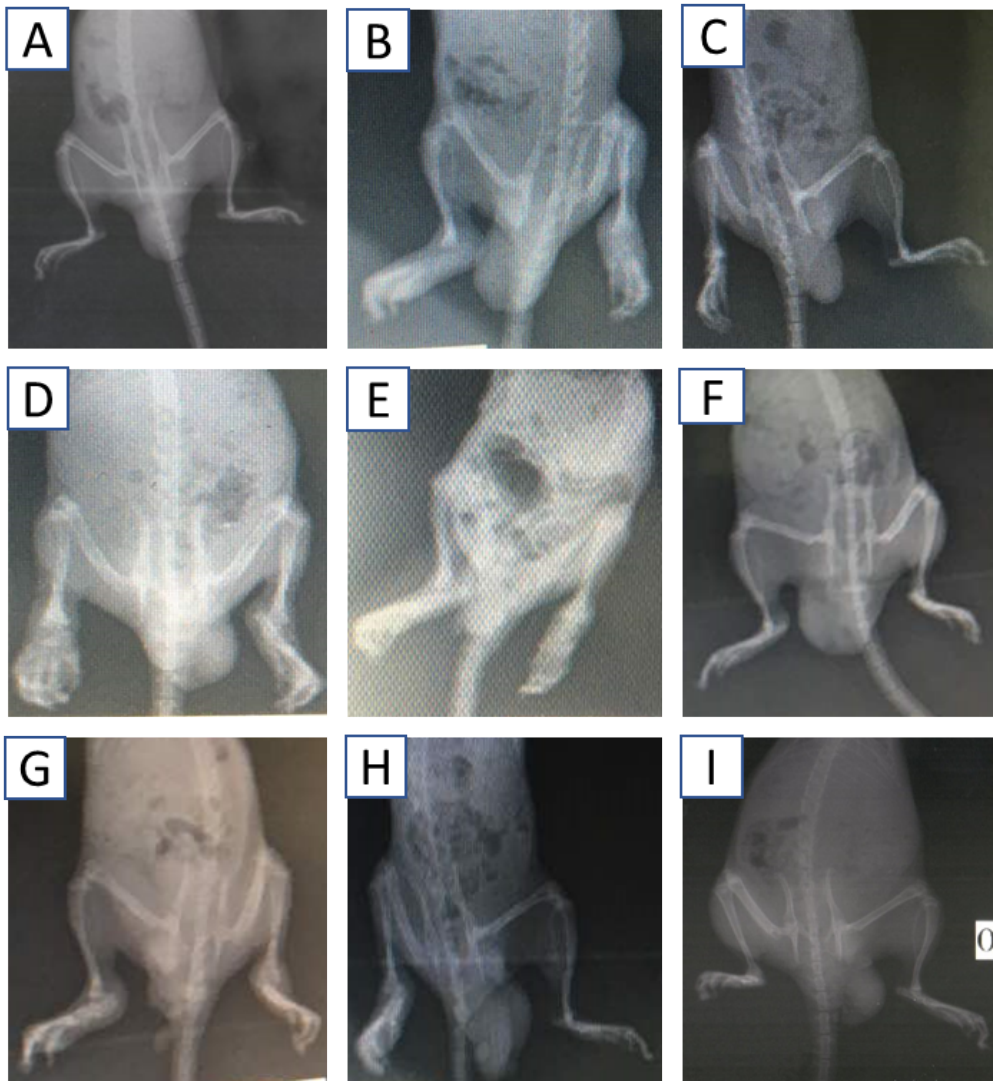

Fig. 7. Radiographs showing the curative effect of **1** and **2** in CFA-induced arthritis in Sprague-Dawley rats. (A)IFA/non-arthritic control, (B)CFA/arthritic control, (C)dexamethasone (3 mg/kg), (D) **1** (3 mg/kg), (E) **1** (10 mg/kg), (F) **1** (30 mg/kg), (G) **2** (3 mg/kg), (H) **2** (10 mg/kg), and (I) **2** (30 mg/kg).

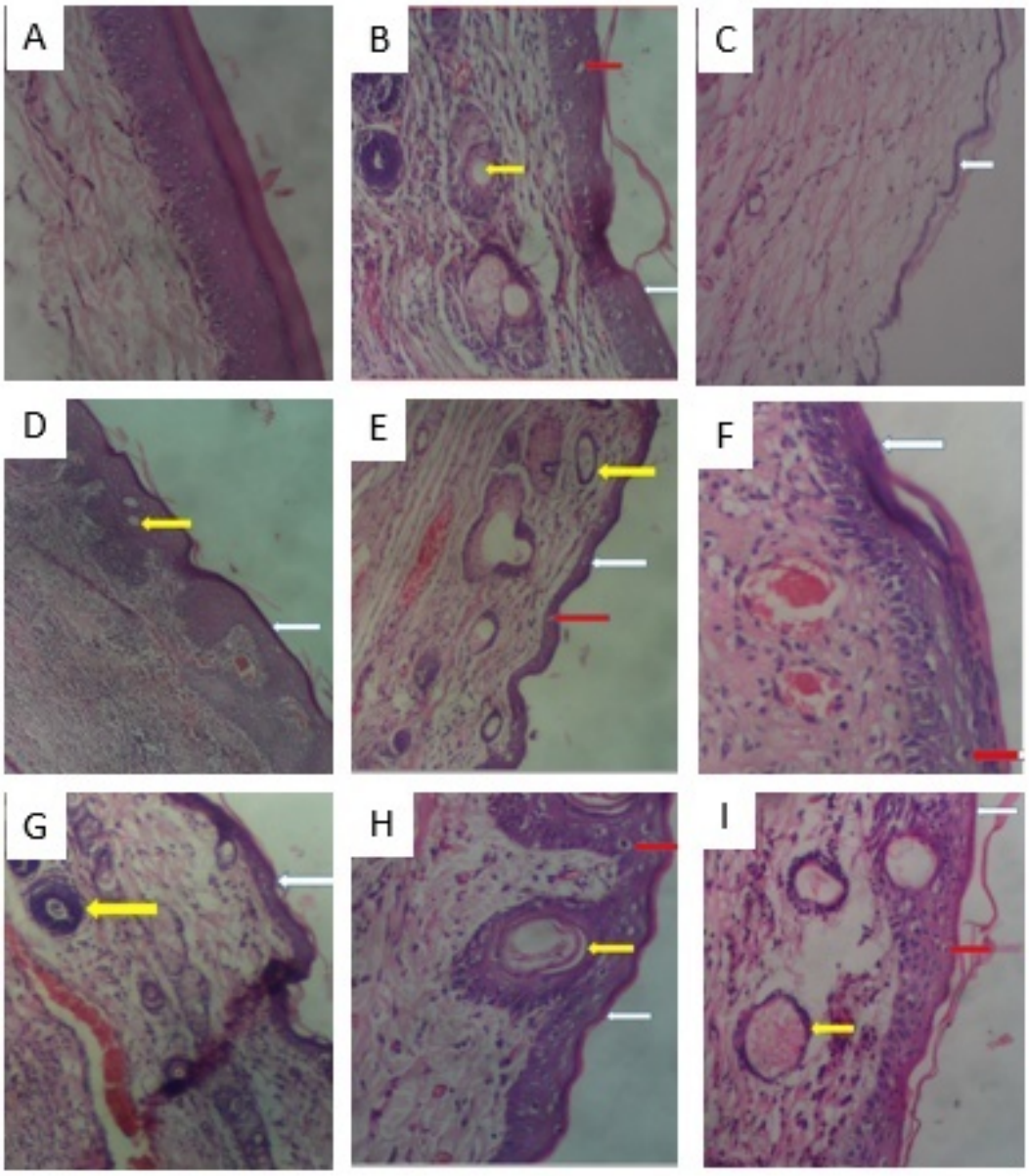

Fig.8. Histopathological examination of rat joints showing the articular cartilage stained with hematoxylin and eosin under a light microscope (× 100)in CFA-induced arthritis in Sprague-Dawley rats. (A) IFA/non-arthritic control, (B) CFA/arthritic control, (C) dexamethasone (3 mg/kg), (D) **1** (3 mg/kg), (E) **1** (10 mg/kg), (F) **1** (30 mg/kg), (G) **2** (3 mg/kg), (H) **2** (10 mg/kg), and (I) **2** (30 mg/kg).

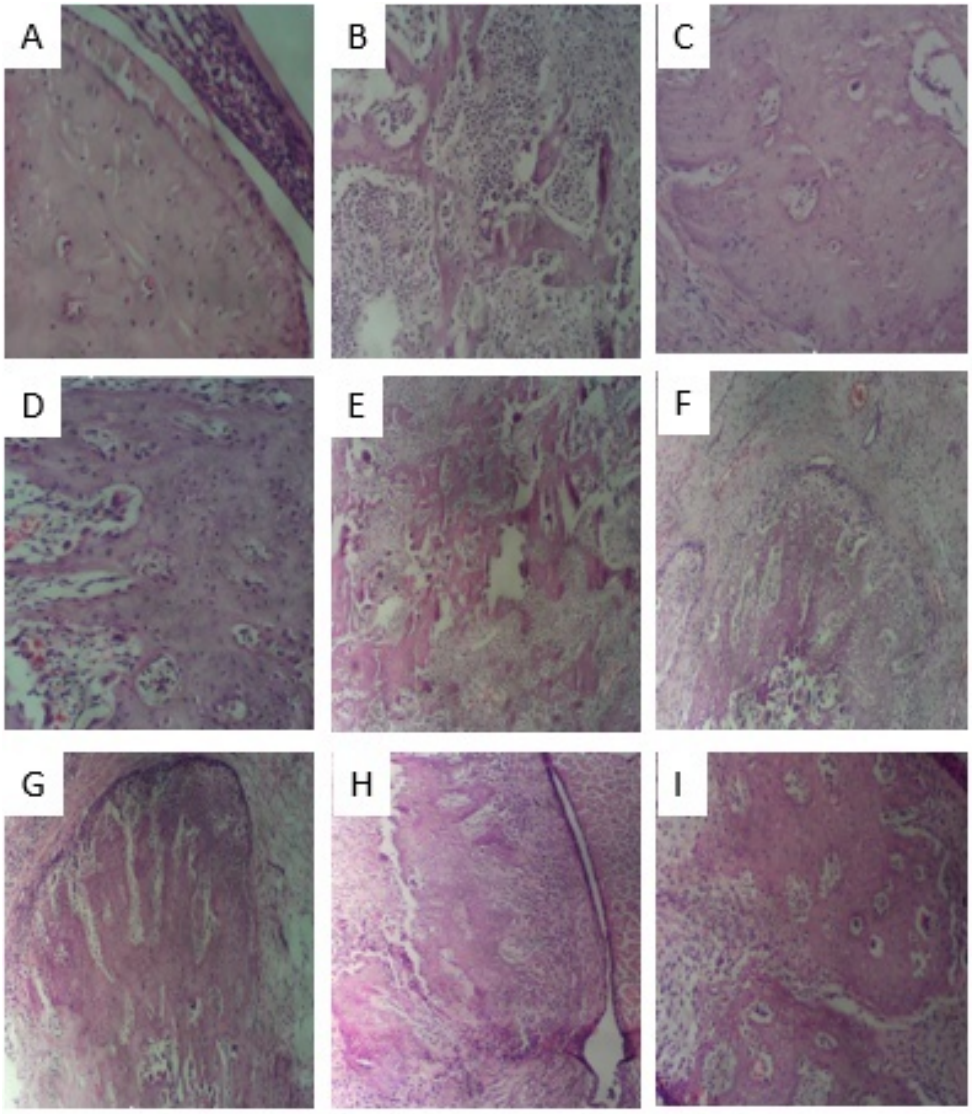

Fig.9. Histopathological examination of rat joints showing the articular bone structure stained with hematoxylin and eosin under a light microscope (× 100)in CFA-induced arthritis in Sprague-Dawley rats. (A)IFA/non-arthritic control, (B)CFA/arthritic control, (C) dexamethasone (3 mg/kg), (D)**1** (3 mg/kg), (E) **1** (10 mg/kg), (F) **1** (30 mg/kg), (G) **2** (3 mg/kg), (H) **2** (10 mg/kg), and (I) **2** (30 mg/kg).

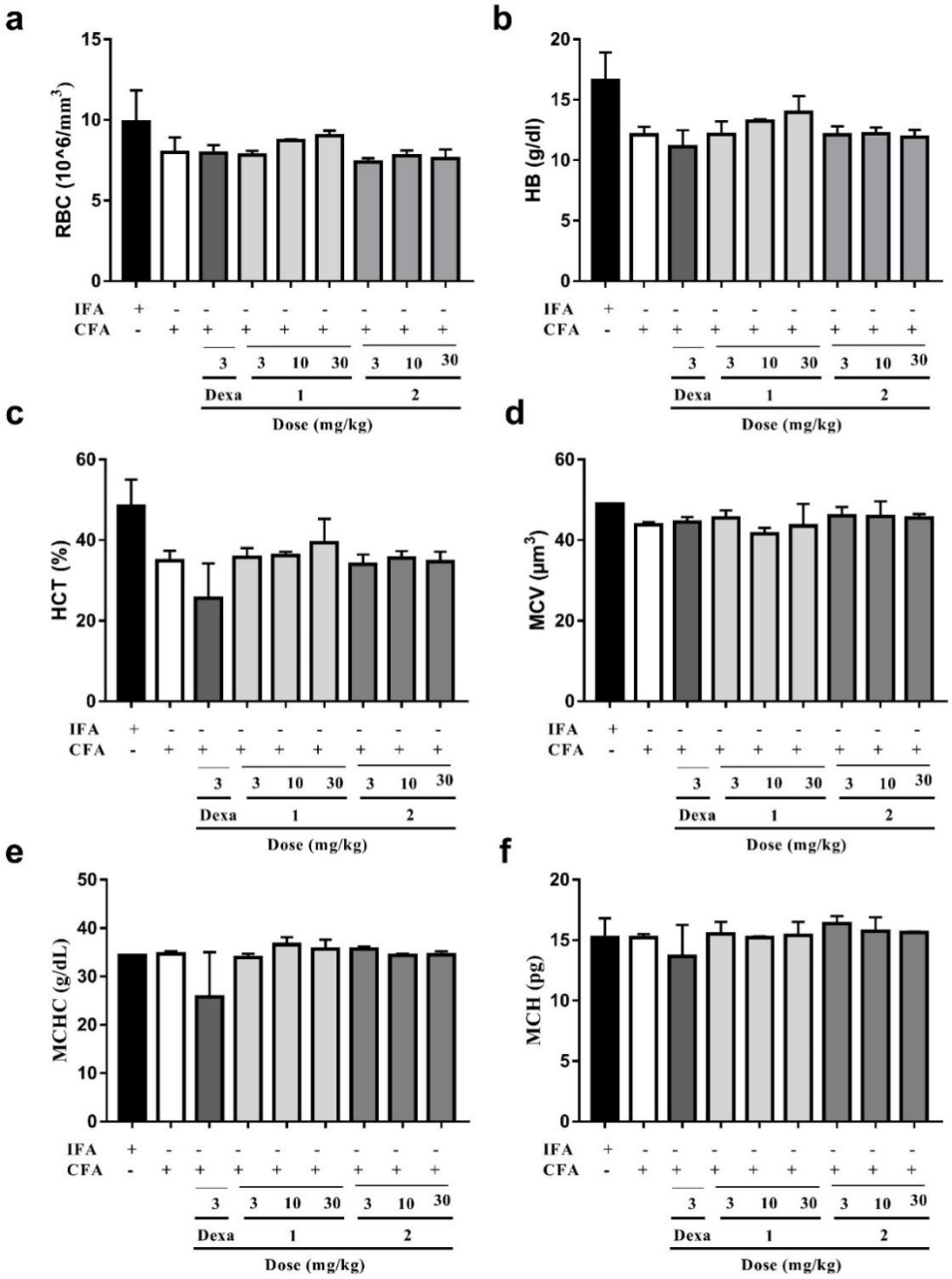

Fig. 10. Effect of dexamethasone, **1** and **2** administration on the hematological parameters in CFA-induced arthritis in Sprague-Dawley rats. Data presented as Mean ± SEM (n = 5). There were no significant differences between arthritic control and treatment groups in any of the red blood cell counts and its related parameters assessed (One-way ANOVA followed by Tukey's post *hoc* test).

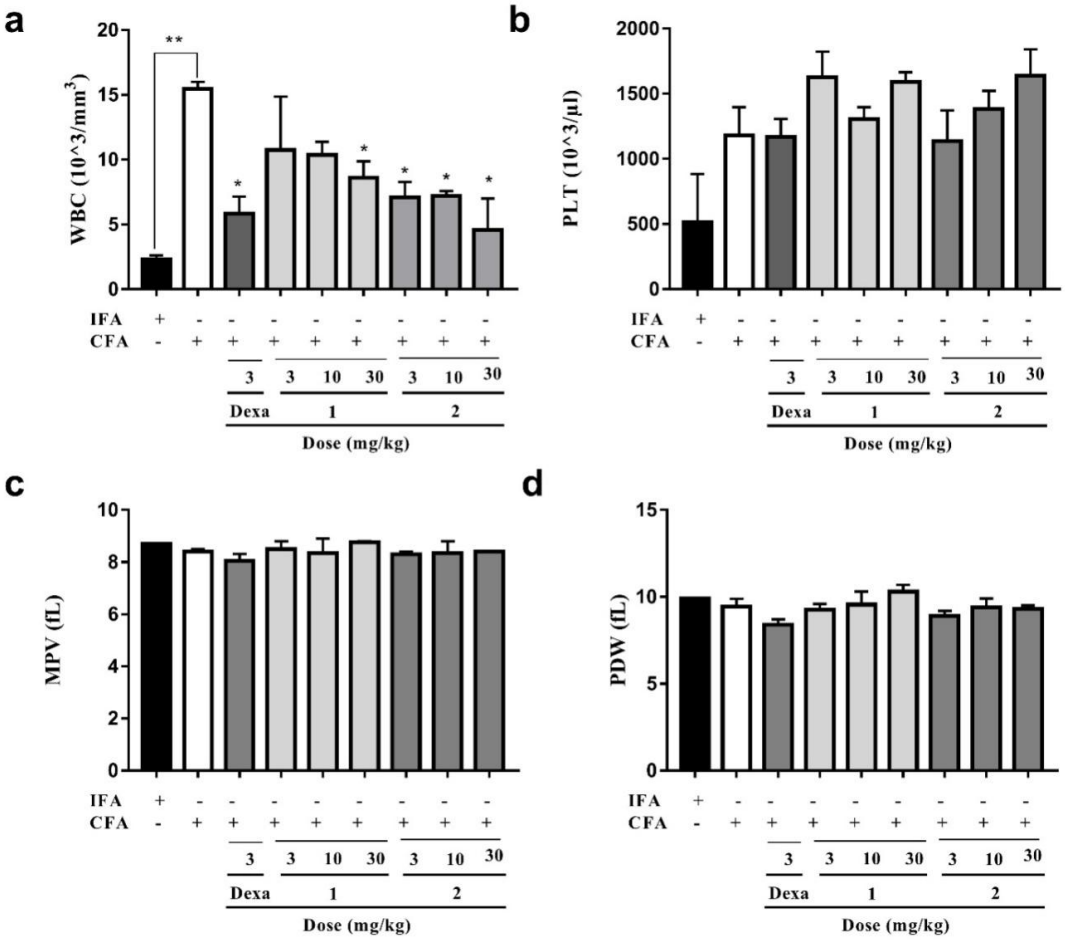

Fig. 11. Effect of dexamethasone, **1** and **2** administration on the hematological parameters in CFA-induced arthritis in Sprague-Dawley rats. Data presented as Mean ± SEM (n = 5). *P<0.05 and **P<0.01, drug treatment groups compared to CFA-treated group(One-way ANOVA followed by Tukey's post *hoc* test).

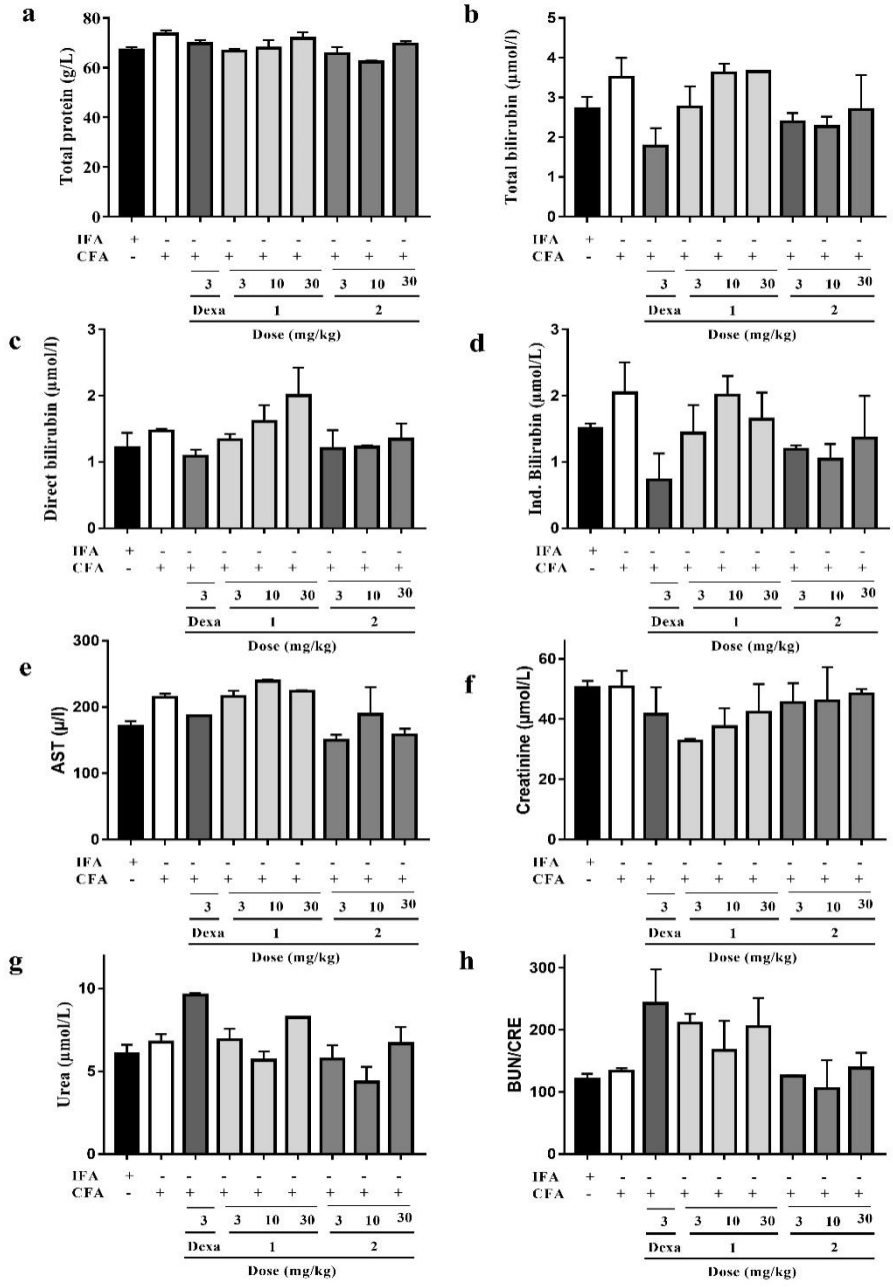

Fig. 12. Effect of dexamethasone, **1** and **2** administration on the serum biochemical parameters in CFA-induced arthritis in Sprague-Dawley rats. Data presented as Mean ± SEM (n = 5). There were no significant differences between arthritic control and treatment groups in any of the biochemical parameters assessed (One-way ANOVA followed by Tukey's post hoc test).

Tables

Table 1. ^{13}CNMR assignments for compounds **1** and **2**[a]

Position	**1**	**2**	Position	**1**	**2**
1	38.75	22.29	16	26.32	36.65
2	27.10	41.53	17	32.65	30.13
3	79.19	213.21	18	47.40	44.26
4	38.94	58.29	19	47.00	29.40
5	55.34	42.07	20	31.24	40.44
6	18.54	41.37	21	34.90	30.29
7	32.82	18.26	22	37.31	35.33
8	41.89	50.75	23	28.56	6.81
9	47.80	37.47	24	15.65	14.67
10	37.12	59.83	25	15.74	18.42
11	23.85	36.18	26	16.97	16.35
12	121.89	29.57	27	26.15	18.11
13	145.35	39.26	28	27.40	31.84
14	39.96	39.20	29	33.49	184.12
15	28.26	29.50	30	23.69	31.53

[a] ^{13}CNMR spectra were obtained at 100 MHz, and recorded in $CDCl_3$ at room temperature.

Table 2. Crystallographic data for compound **2**

Compound	**2**
Formula (with a water molecule)	$C_{30}H_{50}O_4$
Fw	474.43
T (K)	100.00(10)
λ (Å)	1.54184
Crystal system	Monoclinic
Space group	C2
a (Å)	13.33700(7)
b (Å)	6.31317(4)
c (Å)	30.75651(15)
α (°)	90
β (°)	100.3632(5)
γ (°)	90
Volume (Å^3)	2547.41(2)
Z	4
ρ_{calc} (g/cm^3)	1.2377
μ (mm^{-1})	0.620
F (000)	1051.0
Crystal size (mm^3)	0.501 x 0.375 x 0.155
Theta range for data collection (°)	2.92-67.05

Index ranges	-15⩽ h ⩽ 15 -6 ⩽ k ⩽ 7 -36 ⩽ l ⩽ 36
Reflections collected	44153
Independent reflections	4335 [R(int) = 0.0228]
Data completeness (%)	100
Absorption correction	Multi-scan
Refinement method	Olex2.refine, Gauss-Newton minimization
Data / restraints / parameters	4335/ 1 /318
Goodness-of-fit on F^2	1.041
Final R indices [I > 2σ(I)]	R1 = 0.0267 wR2 = 0.0722
R indices (all data)	R1 = 0.0267 wR2 = 0.0722
Largest diff. peak and hole (e. $Å^{-3}$)	0.13 and -0.19